

# Analytical Modelling of a Three-Dimensional (3D) Rectangular Plate Using the Exact Solution Approach

Onyeka, F. C<sup>1</sup>Mama, B. O<sup>2\*</sup> and Nwa-David, C. D<sup>3</sup>

<sup>1</sup>Department of Civil Engineering, Edo State University, Uzairue, Nigeria

<sup>2</sup>Department of Civil Engineering, University of Nigeria, Enugu State, Nigeria

<sup>3</sup>Department of Civil Engineering, Michael Okpara University of Agriculture, Umudike, Nigeria

Corresponding author: benjamine.mama@unn.edu.ng

---

**Abstract:** This study presents a new model used in the stability analysis of a three-dimensional thick rectangular plate that is clamped at the first and second edge, free at the third edge and the other edge simply supported (CCFS) using an exact solution approach. An expression of potential energy of thick plate was formulated using 3D elastic principles thereafter, a compatibility equation of 3D plate was derived through energy equation transformation to get the relations between the rotations and deflection. The solution of compatibility equations yields the exact plates shape function which is derived in terms of trigonometric and polynomial displacement and rotations. Similarly, by minimizing the energy equation with respect to the deflection, the direct governing equation was formulated. The solution of governing equation yields the deflection coefficient of the plate. By minimizing the potential energy equation with respect to deflection coefficient after the action deflection and rotations equation were substituted into it, a more realistic formula for calculation the critical buckling load is established. The proposed method unlike the refined plate theory (RPT), considered all the six stress elements in the analysis. The result showed that the critical buckling loads from the present study using polynomial are slightly higher than those obtained using trigonometric theories signifying the more exactness of the latter. The result of the present study using the established 3-D model for both functions is satisfactory and closer to exact solution compared to 2-D RPT. The overall average percentage differences between the two functions recorded are 2.7%. This shows that at about 97% confidence level, both approaches are the same and can be used with certainty for the analysis of rectangular plate of any thickness.

**Keywords:** uniaxial compressive load, CCFS rectangular plate, stability analysis, 3-D thick plate.

---

Date of Submission: 01-01-2022

Date of Acceptance: 12-01-2022

---

## I. Introduction

Plates are three-dimensional structural elements whose flat, straight and parallel surface is large in relation to the thickness and its use are common to marine, nuclear, structural and road engineering. Plates can be classified based on its support case, such as; simply supported, clamped and free edge boundary conditions. They can be classified according to its shape; rectangular shape, square, circular, circular with a hole, or square with hole, triangular and elliptical. Plates may also be thin, thick or moderately thick depending on their depth [1]. According to [2], a rectangular plate with span-to-depth ratio that is below or exactly twenty ( $a/t \leq 20$ ), can be considered as a thicker plate and considered as a moderately thick plate if the span-to-depth ratio lies between twenty and fifty ( $20 \leq a/t \leq 50$ ).

Thick plates are widely applied in various engineering structures such as; jetties, oil platforms, industrial buildings, bridges, heavy construction equipment, ships, etc., because they possess desirable engineering features which includes extreme fatigue strength, high strength to weight, high stiffness to weight, better tailor ability, low density and excellent corrosion resistance. This has led to increased research interest in thick plates.

The principal analyses for the study of the plates include vibration, buckling and bending analysis [3]. Buckling is the beginning of instability [4]. A plate buckles or becomes elastically unstable as a result of in-plane loading. Achieving the critical buckling loads is the goal of stability analysis of plates. Critical buckling load is the extent of plate instability as a result of axial compressive in-plane forces [5]. Increasing the in-plane compressive load beyond their critical values, results in very large deformations and total plate failure. Although attention has been paid towards stability analysis of plates, much is yet to be done as most work done could not satisfy the exact prescribed boundary conditions or the differential governing equation or both. In order to prevent plate failure, more detailed stability analysis studies are needed.

To analyze thick plates, many researchers employed refined plate theory (RPT) such as the first order shear deformation theory (FSDT) and the higher-order shear deformation plate theory (HSDT). In contrast to the classical plate theory (CPT), these refined plate theories have considered the shear deformation. The refined plate theories, often characterized by the use of trigonometric displacement function, are also limited as they only give an approximate solution while the 3D theory gives an exact solution. A thick plate is a typical three-dimensional element that requires a full 3D analogy [6], hence the necessity of this research work.

The complexity of using double Fourier series and the necessity to simplify complex equations in the thick plate analysis has made researchers to apply energy methods such as Raleigh-Ritz, Galerkin, Work-error and Minimum potential energy [7]. However, most researchers have applied the direct variational method to derive the buckling load without obtaining the actual displacement function by subjecting it to a particular boundary condition. Researchers such as [8, 9 and 10] have used assumed or approximate functions instead of "exact functions" as their shape functions in arithmetic formulations.

In the present study, with the help of the general variational method, the actual displacement function was obtained as the solution of the formulated compatibility equation from the first principle. Similarly, the expression for calculating the critical buckling load was determined using direct variational calculus.

### **Previous Works**

The authors of [5] used polynomial displacement functions to analyze buckling of thick isotropic SSSS rectangular plates. The solutions obtained by the authors were not exact, and a typical 3-D plate theory was not applied. There was also no consideration for a thick plate with CCFS boundary condition.

The study carried out by [11] analyzed the critical buckling load of an SSFS plate with polynomial shape function in Ritz method. The applied shape function was not a derivative of the compatibility equation. Exact solution approach and a rectangular thick plate with the CCFS boundary condition was not also considered by the authors.

The method of finite single Fourier sine transformation was employed by [12] to solve the problem of elastic buckling of the Kirchhoff CCSS rectangular plate. The forces in the thickness axis were not taken into account, therefore, can only predict buckling load of thin and moderately thick plates. In addition, their study failed to cover the plate with the CCFS edge condition.

Using Galerkin's work method, the authors in [13] applied polynomial shape function to derive the equation for buckling of all-round clamped isotropic rectangular plates. For evaluating the coefficients of the critical buckling load, their investigation led to a precise the CCFS boundary condition and moderately thick plate, but cannot be reliably for a typical thick plate analysis. The exact solution approach was also not taken into account neither did they consider a plate with the CCFS boundary condition.

The authors in [14], used a simple and exact approach to analyze rectangular plates with large deflection. Their work showed that when the deflection ratio relative to thickness ( $w/t$ ) is zero, the resulting buckling load concurs with the critical buckling analysis from a small (linear) deflection. However, the authors did not consider the stresses in the direction of thickness axis, therefore can only predict buckling load of thin and moderately thick plates. Also, their work did not consider thick rectangular plates with the CCFS support condition.

In [15], the authors developed a refined trigonometric shear deformation theory for stability analysis of isotropic rectangular plate. Although the theory without using a shear correction factor, has yielded a satisfactory result in the stability analysis, it is not applicable in a typical 3D thick plate analysis. Thick rectangular plates with the CCFS support condition were also not taken into account. The authors assumed trigonometric functions as their displacement functions which made their result not a close-form solution.

The authors in [16] developed exact displacement functions for both buckling and the free vibration analysis of thick rectangular isotropic plates. A typical 3-D thick plate was not covered by their analysis nor did they consider a thick plate of CCFS boundary condition.

To determine the coefficients of the buckling load in a stiffened plate, [17] developed numerical model based on polynomial displacement function. The considerations of authors will not yield a good result when the plate is relatively thick because it is limited to the classical plate theory. A rectangular thick plate of CCFS was not considered by the authors.

Using the refined plate theory, the authors in [18] investigated the stability and vibration behavior of the rectangular thick elastic plate. The stresses in the direction of thickness axis were not considered, hence buckling load of thin and moderately thick plates can only be predicted. The authors also failed to consider the use of exact shape functions and a CCFS plate.

From the study in [19], the authors obtained an analytic solution for the elastic buckling of simply supported thick plates using displacement potential function approach. The displacement function that the authors applied was not derived from the compatibility equation neither did they solve for isotropic rectangular

plates that is clamped at the first and second edge, free at the third edge and the other edge simply supported (CCFS).

Although the authors in [20 and 6] considered a 3D thick plate applying the analytical 3D plate theory for isotropic plates, exact solution approach with exponential deflection function was not used for their buckling analysis neither was CCFS plate considered in their study.

Contrary to the previous works, the distinguishing characteristics of this present study are the method of analysis, type of shape functions, and plates support boundary conditions. Unlike the previous works that assumed the displacement function, the present work obtains the exact formulation from the compatibility equation to get a close form solution of the polynomial and trigonometric displacement functions. Hardly can one see work on the exact solution approach on stability analysis for three dimensional rectangular thick plates using 3D elasticity theory; so this research work is needed. The focus of this study is to perform the stability analysis of a thick rectangular plate that is clamped at the first and second edge, free at the third edge and the other edge simply supported (CCFS).

## II. Methodology

### Potential Energy Equation Formulation

The potential energy of a three dimensional rectangular thick plate is formulated by considering a thick plate assumption that the x-z section and y-z section, which are initially normal to the x-y plane before bending get off normal to the x-y plane after bending of the plate as shown in this section of plate presented in the figure 1.

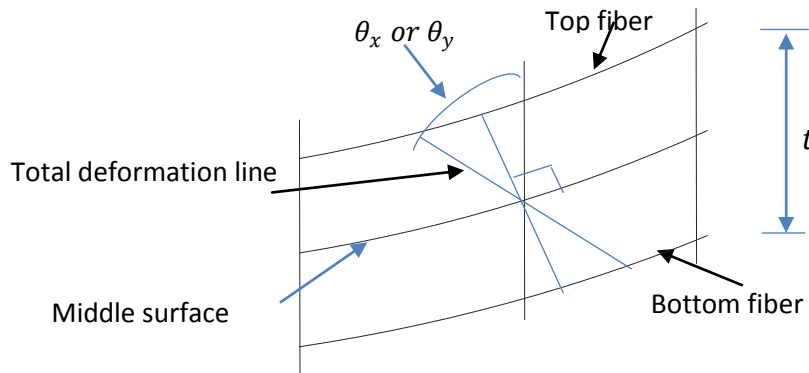


Fig. 1: Rotation of x-z (or y-z) section after bending

The non-dimensional total potential energy  $[\Pi]$  expression for an elastic three-dimensional plate theory of R and Q coordinates at the span-thickness aspect ratio is in line with author in [6] and presented as:

$$\begin{aligned} \Pi = \frac{D^* ab}{2a^2} \int_0^1 \int_0^1 & \left[ (1 - \mu) \left( \frac{\partial \theta_{sx}}{\partial R} \right)^2 + \frac{1}{\beta} \frac{\partial \theta_{sx}}{\partial R} \cdot \frac{\partial \theta_{sy}}{\partial Q} + \frac{(1 - \mu)}{\beta^2} \left( \frac{\partial \theta_{sy}}{\partial Q} \right)^2 + \frac{(1 - 2\mu)}{2\beta^2} \left( \frac{\partial \theta_{sx}}{\partial Q} \right)^2 + \frac{(1 - 2\mu)}{2} \left( \frac{\partial \theta_{sy}}{\partial R} \right)^2 \right. \\ & + \frac{6(1 - 2\mu)}{t^2} \left( a^2 \theta_{sx}^2 + a^2 \theta_{sy}^2 + \left( \frac{\partial w}{\partial R} \right)^2 + \frac{1}{\beta^2} \left( \frac{\partial w}{\partial Q} \right)^2 + 2a \cdot \theta_{sx} \frac{\partial w}{\partial R} + \frac{2a \cdot \theta_{sy}}{\beta} \frac{\partial w}{\partial Q} \right) \\ & \left. + \frac{(1 - \mu)a^2}{t^4} \left( \frac{\partial w}{\partial S} \right)^2 - \frac{N_x}{D} \cdot \left( \frac{\partial w}{\partial R} \right)^2 \right] dR dQ \end{aligned} \quad (1)$$

Where:

$$D^* = \frac{Et^3}{12(1 + \mu)(1 - 2\mu)}$$

### Equation of Equilibrium

The equations of equilibrium in x-z plane y-z plane according the author in [20] is obtained by minimizing the energy equation with respect to rotation in x-z plane and rotation in y-z plane and equate its integrands to zero to get:

$$(1 - \mu) \frac{\partial^2 \theta_{sx}}{\partial R^2} + \frac{1}{2\beta} \cdot \frac{\partial^2 \theta_{sy}}{\partial R \partial Q} + \frac{(1 - 2\mu)}{2\beta^2} \frac{\partial^2 \theta_{sx}}{\partial Q^2} + \frac{6(1 - 2\mu)}{t^2} \left( a^2 \theta_{sx} + a \cdot \frac{\partial w}{\partial R} \right) = 0 \quad (2)$$

$$\frac{1}{2\beta} \cdot \frac{\partial^2 \theta_{sx}}{\partial R \partial Q} + \frac{(1 - \mu)}{\beta^2} \frac{\partial^2 \theta_{sy}}{\partial Q^2} + \frac{(1 - 2\mu)}{2} \frac{\partial^2 \theta_{sy}}{\partial R^2} + \frac{6(1 - 2\mu)}{t^2} \left( a^2 \theta_{sy} + \frac{a \cdot \partial w}{\beta \partial Q} \right) = 0 \quad (3)$$

Using law of addition, the Equations 2 and 3 will be simplified, then factorizing the outcome gives:

$$\frac{\partial w}{\partial R} \left[ (1 - \mu) \frac{\partial^2}{\partial R^2} + \frac{1}{\beta^2} \cdot \frac{\partial^2}{\partial Q^2} (1 - \mu) + \frac{6(1 - 2\mu)a^2}{t^2} \cdot \left( 1 + \frac{1}{c} \right) \right] = 0 \quad (4)$$

$$\frac{1}{\beta} \cdot \frac{\partial w}{\partial Q} \left[ \frac{\partial^2}{\partial R^2} (1 - \mu) + \frac{(1 - \mu)}{\beta^2} \cdot \frac{\partial^2}{\partial Q^2} + \frac{6(1 - 2\mu)a^2}{t^2} \cdot \left( 1 + \frac{1}{c} \right) \right] = 0 \quad (5)$$

After simplification using law of addition, one of the possible of Equation becomes:

$$\frac{6(1 - 2\mu)(1 + c)}{t^2} = - \frac{c(1 - \mu)}{a^2} \left( \frac{\partial^2}{\partial R^2} + \frac{1}{\beta^2} \frac{\partial^2}{\partial Q^2} \right) \quad (6)$$

**General Governing Equation**

The minimization of energy equation with respect to deflection gives the general governing equation as presented in [21]:

$$\frac{D^*}{2a^2} \int_0^1 \int_0^1 \left[ \frac{6(1 - 2\mu)(1 + c)}{t^2} \left( \frac{\partial^2 w}{\partial R^2} + \frac{1}{\beta^2} \cdot \frac{\partial^2 w}{\partial Q^2} \right) + \frac{(1 - \mu)a^2}{t^4} \frac{\partial^2 w}{\partial S^2} - \frac{N_x}{D^*} \cdot \frac{\partial^2 w}{\partial R^2} \right] dR dQ = 0 \quad (7)$$

Substituting Equation 6 into Equation 7 and simplifying the outcome gives two governing differential equations of a 3-D rectangular plate subject to pure buckling as presented in Equation 8 and 9:

$$\frac{\partial^4 w_1}{\partial R^4} + \frac{2}{\beta^2} \cdot \frac{\partial^4 w_1}{\partial R^2 \partial Q^2} + \frac{1}{\beta^4} \cdot \frac{\partial^4 w_1}{\partial Q^4} - \frac{N_{x1} a^4}{g D^*} \cdot \frac{\partial^2 w_1}{\partial R^2} = 0 \quad (8)$$

$$\frac{(1 - \mu)a^4}{t^4} \cdot \frac{\partial^2 w_S}{\partial S^2} - \frac{N_{xs} a^4}{D^*} \cdot \frac{\partial^2 w_S}{\partial R^2} = 0 \quad (9)$$

Thus, the trigonometric and polynomial expression for deflection derived from Equation (8) is given in Equation (10) and (11) respectively as:

$$w = (a_0 + a_1 R + a_2 \cos g_1 R + a_3 \sin g_1 R) \times (b_0 + b_1 Q + b_2 \cos g_2 Q + b_3 \sin g_2 Q) \quad (10)$$

$$w = \Delta_0 (a_0 + a_1 R + a_2 R^2 + a_3 R^3 + a_4 R^4) \times (b_0 + b_1 Q + b_2 Q^2 + b_3 Q^3 + b_4 Q^4) \quad (11)$$

Equation (10a) and (10b) can be re-written as:

$$w = A_1 h \quad (12)$$

Given that h and A<sub>1</sub> are the plates shape function and coefficient of deflection, where:

$$A_1 = \Delta_0 \begin{bmatrix} a_0 \\ a_1 \\ a_2 \\ a_3 \\ a_4 \end{bmatrix} \cdot \begin{bmatrix} b_0 \\ b_1 \\ b_2 \\ b_3 \\ b_4 \end{bmatrix} \quad (13)$$

$$h = (1 R \cos g_1 R \sin g_1 R) \times (1 Q \cos g_2 Q \sin g_2 Q) \quad (14)$$

and;

$$h = [1 R R^2 R^3 R^4] \cdot [1 Q Q^2 Q^3 Q^4] \quad (15)$$

Recall [6]:

$$\theta_{sx} = \frac{A_2}{a} \cdot \frac{\partial h}{\partial R} \quad (16)$$

$$\theta_{sy} = \frac{A_3}{a\beta} \cdot \frac{\partial h}{\partial Q} \quad (17)$$

Given that: A<sub>1</sub> is the coefficient of deflection A<sub>2</sub> and A<sub>3</sub> are the coefficients of shear deformation in x axis and y axis respectively.

**Direct Governing Equation**

By substituting Equations (12), (16) and (17) into Equation (1), the Energy equation becomes:

$$\begin{aligned} \Pi = \frac{D^* ab}{2a^4} & \left[ (1 - \mu) A_2^2 \int_0^1 \int_0^1 \left( \frac{\partial^2 h}{\partial R^2} \right)^2 dR dQ + \frac{1}{\beta^2} \left[ A_2 \cdot A_3 + \frac{(1 - 2\mu) A_2^2}{2} + \frac{(1 - 2\mu) A_3^2}{2} \right] \int_0^1 \int_0^1 \left( \frac{\partial^2 h}{\partial R \partial Q} \right)^2 \right. \\ & + \frac{(1 - \mu) A_3^2}{\beta^4} \int_0^1 \int_0^1 \left( \frac{\partial^2 h}{\partial Q^2} \right)^2 dR dQ \\ & + 6(1 - 2\mu) \left( \frac{a}{t} \right)^2 \left( [A_2^2 + A_1^2 + 2A_1 A_2] \cdot \int_0^1 \int_0^1 \left( \frac{\partial h}{\partial R} \right)^2 dR dQ \right. \\ & \left. \left. + \frac{1}{\beta^2} \cdot [A_3^2 + A_1^2 + 2A_1 A_3] \cdot \int_0^1 \int_0^1 \left( \frac{\partial h}{\partial Q} \right)^2 dR dQ \right) - \frac{N_x a^2 A_1^2}{D^*} \cdot \int_0^1 \int_0^1 \left( \frac{\partial h}{\partial R} \right)^2 dR dQ \right] \quad (18) \end{aligned}$$

Differentiating Equation (18) with respect to shear deformation coefficient ( $A_2$  and  $A_3$ ), and solve simultaneously gives:

$$A_2 = \left( \frac{k_{12}k_{23} - k_{13}k_{22}}{k_{12}k_{12} - k_{11}k_{22}} \right) \cdot A_1 \quad (19)$$

$$A_3 = \left( \frac{k_{12}k_{13} - k_{11}k_{23}}{k_{12}k_{12} - k_{11}k_{22}} \right) \cdot A_1 \quad (20)$$

Let:

$$k_{11} = (1 - \mu)k_{RR} + \frac{1}{2\beta^2}(1 - 2\mu)k_{RQ} + 6(1 - 2\mu) \left( \frac{a}{t} \right)^2 k_R \quad (21)$$

$$k_{21} = k_{12} = \frac{1}{2\beta^2}k_{RQ}; \quad k_{13} = -6(1 - 2\mu) \left( \frac{a}{t} \right)^2 k_R; \quad k_{32} = k_{23} = -\frac{6}{\beta^2}(1 - 2\mu) \left( \frac{a}{t} \right)^2 k_Q \quad (22)$$

$$k_{22} = \frac{(1 - \mu)}{\beta^4}k_{QQ} + \frac{1}{2\beta^2}(1 - 2\mu)k_{RQ} + \frac{6}{\beta^2}(1 - 2\mu) \left( \frac{a}{t} \right)^2 k_Q \quad (23)$$

Where:

$$k_{RR} = \int_0^1 \int_0^1 \left( \frac{\partial^2 h}{\partial R^2} \right)^2 dRdQ \quad (24)$$

$$k_{RQ} = \int_0^1 \int_0^1 \left( \frac{\partial^2 h}{\partial R \partial Q} \right)^2 dRdQ \quad (25)$$

$$k_{QQ} = \int_0^1 \int_0^1 \left( \frac{\partial^2 h}{\partial Q^2} \right)^2 dRdQ \quad (26)$$

$$k_R = \int_0^1 \int_0^1 \left( \frac{\partial h}{\partial R} \right)^2 dRdQ \quad (27)$$

$$k_Q = \int_0^1 \int_0^1 \left( \frac{\partial h}{\partial Q} \right)^2 dRdQ \quad (28)$$

Differentiating Equation (18) with respect to deflection coefficient ( $A_1$ ) and simplifying the outcome, an expression for the critical buckling load ( $N_{xcr}$ ) is established as:

$$\frac{N_x a^2}{D^*} = 6(1 - 2\mu) \left( \frac{a}{t} \right)^2 \left( \left[ 1 + \left( \frac{k_{12}k_{23} - k_{13}k_{22}}{k_{12}k_{12} - k_{11}k_{22}} \right) \right] + \frac{1}{\beta^2} \cdot \left[ 1 + \left( \frac{k_{12}k_{13} - k_{11}k_{23}}{k_{12}k_{12} - k_{11}k_{22}} \right) \right] \cdot \frac{k_Q}{k_R} \right) \quad (29)$$

Similarly:

$$N_{xcr} = \frac{(1 + \mu)Et^3}{2a^2} \left( \frac{a}{t} \right)^2 \left( \left[ 1 + \left( \frac{k_{12}k_{23} - k_{13}k_{22}}{k_{12}k_{12} - k_{11}k_{22}} \right) \right] + \frac{1}{\beta^2} \cdot \left[ 1 + \left( \frac{k_{12}k_{13} - k_{11}k_{23}}{k_{12}k_{12} - k_{11}k_{22}} \right) \right] \cdot \frac{k_Q}{k_R} \right) \quad (30)$$

### Numerical Analysis

An example of a thick rectangular plate that is clamped at the first and second edge, free at the third edge and the other edge simply supported (CCFS) subjected to uniaxial compressive load is presented. The trigonometric and polynomial displacement function as presented in the Equation (10) and (11) was applied to determine the value of the critical buckling load in the plate at various aspect ratios.

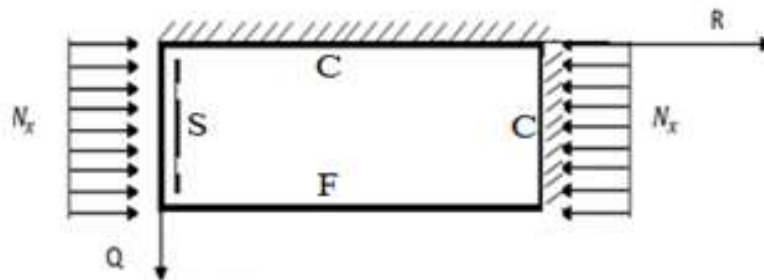


Figure 2: CCFS Rectangular Plate subjected to uniaxial compressive load

The boundary conditions of the plate in figure 3 are as follows:

$$\text{At } R = Q = 0; \text{ deflection } (w) = 0 \quad (31)$$

At  $R = 0$ , slope  $\left(\frac{dw}{dR}\right)$ ;  $Q = 0$ , slope  $\left(\frac{dw}{dQ}\right) = 0$  (32)

At  $R = 1$ , deflection  $(w) = 0$ ;  $Q = 1$ , bending moment  $\left(\frac{d^2w}{dQ^2}\right) = 0$  (33)

At  $R = 1$ , bending moment  $\left(\frac{d^2w}{dR^2}\right) = 0$ ;  $Q = 1$ , shear force  $\left(\frac{d^3w}{dQ^3}\right) = 0$  (34)

At  $Q = 1$ , slope  $\left(\frac{dw}{dQ}\right) = \frac{2}{3b_5}$  (35)

Substituting Equation (31) to (35) into the derivatives of  $w$  and solving gave the characteristic equation as:

$g_1 \cos g_1 - \sin g_1 = 0$ ;  $b_2 \cos g_1 = 0$  (36)

The value of  $g_1$  that satisfies Equation (36) is:

$g_1 = 4.49340946$ ;  $g_1 = \frac{n\pi}{2}$  [where  $n = 1, 2, 3 \dots$ ] (37)

Substituting Equation (37) into the derivatives of  $w$  and satisfying the boundary conditions of Equation (31) to (35) gives the following constants:

$a_0 = g_1 a_3$ ;  $a_1 = -g_1 a_3$ ;  $a_2 = -g_1 a_3$ ;  $b_3 = 0$ ;  $b_1 = -g_1 b_3 = 0$ ;  $b_0 = -b_2$  (38)

Substituting the constants of Equation (36) and (38) into Equation (10) and simplify the outcome gives:

$w = a_3(g_1 - g_1 R - g_1 \cos g_1 R + \sin g_1 R) \times b_0 \left(1 - \cos \frac{n\pi Q}{2}\right)$  (39)

Thus:

$w = a_3 \times b_2(g_1 - g_1 R - g_1 \cos g_1 R + \sin g_1 R) \cdot \left(\cos \frac{\pi Q}{2} - 1\right)$  (40)

Let the amplitude,

$A_1 = a_3 \times b_2$  (41)

And;

$h = (g_1 - g_1 R - g_1 \cos g_1 R + \sin g_1 R) \cdot \left(\cos \frac{\pi Q}{2} - 1\right)$  (42)

Thus, the trigonometric deflection functions after satisfying the boundary conditions is:

$w = A_1(g_1 - g_1 R - g_1 \cos g_1 R + \sin g_1 R) \cdot \left(\cos \frac{\pi Q}{2} - 1\right)$  (43)

Similarly, substituting Equations (31 to 34) into Equation (11) and solving gives the following constants:

$a_0 = 0$ ;  $a_1 = 0$ ;  $a_2 = 1.5a_4$ ;  $a_3 = -2.5a_4$  and (44)

$b_0 = 0$ ;  $b_1 = 0$ ;  $b_2 = 2.8b_5$ ;  $b_3 = -5.2b_5$ ;  $b_4 = 3.8b_5$  (45)

Substituting the constants of Equation (44) and (45) into Equation (11) gives;

$w = (1.5a_4 R^2 - 2.5a_4 R^3 + a_4 R^4) \times (2.8b_5 Q^2 - 5.2b_5 Q^3 + 3.8b_5 Q^4 - Q^5)$  (46)

Simplifying Equation (46) which satisfying the boundary conditions of Equation (31 to 34) gives:

$w = a_4(1.5R^2 - 2.5R^3 + R^4) \times b_5(2.8Q^2 - 5.2Q^3 + 3.8Q^4 - Q^5)$  (47)

Thus:

$w = a_4 \times b_5(1.5R^2 - 2.5R^3 + R^4) \times (2.8Q^2 - 5.2Q^3 + 3.8Q^4 - Q^5)$  (48)

Let the amplitude,

$A_1 = a_4 \times b_5$  (49)

And;

$h = (1.5R^2 - 2.5R^3 + R^4) \times (2.8Q^2 - 5.2Q^3 + 3.8Q^4 - Q^5)$  (50)

Thus, the polynomial deflection functions after satisfying the boundary conditions is:

$w = (1.5R^2 - 2.5R^3 + R^4) \times (2.8Q^2 - 5.2Q^3 + 3.8Q^4 - Q^5) \cdot A_1$  (51)

Thus, a numerical values of the stiffness for a CCFS plate were obtained using Equation (24) to (28) by applying the two shape function (trigonometric and polynomial) as obtained in Equation (42) and Equation (50) and their results are presented in Table 1.

**Table 1:** The polynomial and trigonometric stiffness coefficients of deflection function of the CCFS plate

Displacement Shape Function	$k_{RR}$	$k_{RQ}$	$k_{QQ}$	$k_R$	$k_Q$
Polynomial	0.123179	0.016218	0.019715	0.005866	0.001427
Trigonometric	942.4073	253.8195	58.01520	46.65332	47.02532

### III. Results and Discussions

The result of the numerical example is presented in this section which was obtained using the equation of the critical buckling load of the plate as shown in the Equation (29) and (30). The non-dimensional value of the critical buckling load for an isotropic thick rectangular plate that is clamped at the first and second edge, free of support at third edge and simply supported at the fourth edge (CCFS) under uniaxial compressive load at varying aspect ratio is presented in Table 2, 3, 4 and 5. This result was obtained using the two models (trigonometric and polynomial) to determine the critical buckling load of the plate. Also, a numerical and graphical comparison was made between the two models (trigonometric and polynomial functions) to study plate's stability at varying thickness and aspect ratio (see table 6 and figure 3 to 11).

The values obtained in Table 2, 3, 4 and 5, shows that as the values of critical buckling load increase, the span- thickness ratio increases. This reveals that as the in-plane load on the plate increase and approaches the critical buckling, the failure in a plate structure is a bound to occur. This means that a decrease in the thickness of the plate, increases the chance of failure in a plate structure. Hence, failure tendency in the plate structure can be mitigated by increasing its thickness.

It is also observed in the table that as the length to breadth ratio of the increases, the value of critical buckling load decreases while as critical buckling load increases, the length to breadth ratio increases. This implies that an increase in plate width increases the chance of failure in a plate structure. It can be deduced that as the in-plane load which will cause the plate to fail by compression increases from zero to critical buckling load, the buckling of the plate exceed specified elastic limit thereby causing failure in the plate structure. This means that, the load that causes the plate to deform also causes the plate material to buckle simultaneously.

The comparison shows that at an aspect ratio of 1.0, 1.5, 2.0, 2.5, the trigonometric model predicts a slightly higher value of the critical buckling load than polynomial function, whereas at an aspect ratio of 3.0, 3.5, 4.0, 4.5 5.0, the polynomial model predicts a slightly higher value of the critical buckling load than trigonometric function. Meanwhile, the trigonometric function gives higher value of stiffness coefficient is than polynomial, however the result of critical load obtained using both models are very close when analyzed using the percentage difference evaluation.

The percentage difference of critical buckling load between the present study using polynomial, and that of trigonometric function for an isotropic CCFS thick rectangular plate subjected to a uniaxial compression at a varying aspect ratio is presented in table 6 and figures 3 to 11. It was discovered that the values of percentage error increase as the span to thickness ratio of the plate increases, the percentage differences between the two approaches reduce as the span to thickness ratio reduced. This means that as the plate gets thinner, the two methods differs more and becomes close as the plate gets thick. This shows the high level of convergence between the two approaches for a thicker plate shows high level of accuracy and reliability of this model in the thick plate analysis and can also be used in confidence for analysis of all rectangular plate analysis.

The lowest average percentage difference is 0.1448 and 0.9342 which occur in an aspect ratio and the highest average percentage difference is 7.7803 which occur in an aspect ratio of one (1). This shows that, the degree of error in percentage between the two models increases as the length to breadth ratio decreases. This means that as the length of the plate widens, the two models (trigonometric and polynomial) becomes closer. The graph shows that at an aspect ratio of 2.5 the two models gives almost the same value of buckling load (see Figure 6).

In summary, the overall average percentage differences between the two functions recorded is 2.7%. These differences being less than 7% are quite acceptable in statistical analysis, as it will not put the structure into danger. This means that at about 97% confidence both approaches are the same and can be applied with confidence for analysis of plate of any thickness. Thus, the present model has some level safety and can be used with confidence for buckling analysis of the CSFS boundary condition.

### IV. Conclusion and Recommendation

The 3-D exact theory is a plate theory that involves all the six strains ( $\epsilon_x, \epsilon_y, \epsilon_z, \gamma_{xy}, \gamma_{xz}$  and  $\gamma_{yz}$ ) and stress ( $\sigma_x, \sigma_y, \sigma_z, \tau_{xy}, \tau_{xz}$  and  $\tau_{yz}$ ) components in the analysis. Hence, they include more modulus of elasticity (E) and other mechanical properties of the plate. As a consequence, the proposed 3-D approach always predicts buckling load greater than those predicted by CPT, FSDT and higher-order RPT because of these additional load (stresses), modulus of elasticity (E) and other mechanical properties of the plate.

From the result of percentage difference recorded, it can be concluded that the trigonometric displacement function developed to give a close form solution, thereby considered more accurate and safe for complete exact three-dimensional thick plate analysis than the polynomial. Its use in the analysis of thick plates will yield almost an exact result. On the other hand, the polynomial displacement function which predicts a slightly higher value of average percentage difference gives an approximate solution whose exact value is tends to infinity. Thus, confirming that the exact 3-D plate theory using polynomial and trigonometric displacement

function provides a good solution for the stability analysis of plates and, can be recommended for analysis of any type of rectangular plate under the same loading and boundary condition.

**Table 2:** Non-dimensional critical buckling load  $\frac{N_x a^2}{\pi^2 D}$  on the CCFS rectangular plate using trigonometric function

$\alpha = \frac{a}{t}$	$N_{xcr} = \frac{N_x a^2}{\pi^2 D}$								
	$\beta = 1.0$	$\beta = 1.5$	$\beta = 2.0$	$\beta = 2.5$	$\beta = 3.0$	$\beta = 3.5$	$\beta = 4.0$	$\beta = 4.5$	$\beta = 5.0$
4	2.7603	2.1766	1.9856	1.8995	1.8534	1.8258	1.8079	1.7957	1.7870
5	3.0319	2.3860	2.1751	2.0802	2.0293	1.9989	1.9792	1.9658	1.9562
10	3.4953	2.7391	2.4933	2.3829	2.3238	2.2885	2.2657	2.2501	2.2390
15	3.5979	2.8165	2.5629	2.4490	2.3881	2.3517	2.3281	2.3121	2.3006
20	3.6353	2.8447	2.5882	2.4730	2.4114	2.3746	2.3508	2.3346	2.3230
30	3.6625	2.8652	2.6066	2.4905	2.4284	2.3912	2.3673	2.3509	2.3392
40	3.6721	2.8724	2.6131	2.4967	2.4344	2.3971	2.3731	2.3567	2.3450
50	3.6766	2.8758	2.6161	2.4995	2.4371	2.3999	2.3758	2.3594	2.3476
60	3.6790	2.8776	2.6177	2.5011	2.4387	2.4014	2.3773	2.3608	2.3491
70	3.6805	2.8787	2.6187	2.5020	2.4396	2.4023	2.3782	2.3617	2.3500
80	3.6815	2.8794	2.6194	2.5026	2.4402	2.4028	2.3787	2.3623	2.3505
90	3.6821	2.8799	2.6198	2.5030	2.4406	2.4032	2.3791	2.3627	2.3509
100	3.6826	2.8803	2.6201	2.5033	2.4409	2.4035	2.3794	2.3629	2.3512
1000	3.6846	2.8818	2.6215	2.5046	2.4421	2.4047	2.3806	2.3641	2.3524
1500	3.6846	2.8818	2.6215	2.5046	2.4421	2.4047	2.3806	2.3641	2.3524

**Table 3:** Non-dimensional critical buckling load  $\frac{N_x a^2}{Et^3}$  on the CCFS rectangular plate using trigonometric function

$\alpha = \frac{a}{t}$	$N_{xcr} = \frac{N_x a^2}{Et^3}$								
	$\beta = 1.0$	$\beta = 1.5$	$\beta = 2.0$	$\beta = 2.5$	$\beta = 3.0$	$\beta = 3.5$	$\beta = 4.0$	$\beta = 4.5$	$\beta = 5.0$
4	2.4216	1.9095	1.7420	1.6664	1.6260	1.6017	1.5861	1.5754	1.5678
5	2.6599	2.0932	1.9082	1.8249	1.7803	1.7536	1.7364	1.7246	1.7162
10	3.0664	2.4030	2.1874	2.0905	2.0387	2.0077	1.9877	1.9740	1.9643
15	3.1564	2.4709	2.2484	2.1485	2.0951	2.0631	2.0425	2.0284	2.0183
20	3.1892	2.4957	2.2706	2.1696	2.1155	2.0832	2.0624	2.0481	2.0379
30	3.2131	2.5136	2.2868	2.1849	2.1304	2.0978	2.0768	2.0624	2.0522
40	3.2216	2.5200	2.2925	2.1903	2.1357	2.1030	2.0819	2.0675	2.0572
50	3.2255	2.5229	2.2951	2.1928	2.1381	2.1054	2.0843	2.0699	2.0596
60	3.2276	2.5245	2.2965	2.1942	2.1394	2.1067	2.0856	2.0711	2.0608
70	3.2289	2.5255	2.2974	2.1950	2.1402	2.1075	2.0864	2.0719	2.0616
80	3.2297	2.5261	2.2980	2.1956	2.1408	2.1080	2.0869	2.0724	2.0621
90	3.2303	2.5266	2.2984	2.1959	2.1411	2.1084	2.0872	2.0728	2.0625
100	3.2307	2.5269	2.2986	2.1962	2.1414	2.1086	2.0875	2.0730	2.0627
1000	3.2325	2.5282	2.2998	2.1973	2.1424	2.1097	2.0885	2.0740	2.0637
1500	3.2325	2.5282	2.2998	2.1973	2.1425	2.1097	2.0885	2.0741	2.0637

**Table 4:** Non-dimensional critical buckling load  $\frac{N_x a^2}{\pi^2 D}$  on the CCFS rectangular plate using polynomial function

$\alpha = \frac{a}{t}$	$N_{xcr} = \frac{N_x a^2}{\pi^2 D}$								
	$\beta = 1.0$	$\beta = 1.5$	$\beta = 2.0$	$\beta = 2.5$	$\beta = 3.0$	$\beta = 3.5$	$\beta = 4.0$	$\beta = 4.5$	$\beta = 5.0$
4	2.4790	2.0504	1.9300	1.8803	1.8551	1.8404	1.8312	1.8249	1.8205
5	2.7496	2.2572	2.1214	2.0656	2.0373	2.0209	2.0105	2.0036	1.9987
10	3.2183	2.6080	2.4447	2.3781	2.3445	2.3250	2.3127	2.3044	2.2985
15	3.3232	2.6853	2.5157	2.4467	2.4118	2.3916	2.3789	2.3703	2.3642
20	3.3615	2.7134	2.5415	2.4717	2.4363	2.4159	2.4029	2.3942	2.3881
30	3.3894	2.7339	2.5603	2.4898	2.4541	2.4335	2.4204	2.4117	2.4055
40	3.3993	2.7411	2.5670	2.4962	2.4604	2.4397	2.4266	2.4178	2.4116
50	3.4039	2.7445	2.5700	2.4992	2.4633	2.4426	2.4295	2.4207	2.4145
60	3.4064	2.7463	2.5717	2.5008	2.4649	2.4442	2.4311	2.4222	2.4160
70	3.4079	2.7474	2.5727	2.5018	2.4659	2.4451	2.4320	2.4232	2.4169
80	3.4089	2.7482	2.5734	2.5024	2.4665	2.4457	2.4326	2.4238	2.4176
90	3.4096	2.7487	2.5738	2.5029	2.4669	2.4462	2.4330	2.4242	2.4180
100	3.4101	2.7490	2.5742	2.5032	2.4672	2.4465	2.4333	2.4245	2.4183
1000	3.4121	2.7505	2.5755	2.5045	2.4685	2.4477	2.4346	2.4258	2.4195
1500	3.4121	2.7505	2.5755	2.5045	2.4685	2.4477	2.4346	2.4258	2.4195

**Table 5:** Non-dimensional critical buckling load  $\frac{N_x a^2}{E t^3}$  on the CCFS rectangular plate using polynomial function

$\alpha = \frac{a}{t}$	$N_{xcr} = \frac{N_x a^2}{E t^3}$								
	$\beta = 1.0$	$\beta = 1.5$	$\beta = 2.0$	$\beta = 2.5$	$\beta = 3.0$	$\beta = 3.5$	$\beta = 4.0$	$\beta = 4.5$	$\beta = 5.0$
4	2.1748	1.7988	1.6932	1.6496	1.6274	1.6146	1.6065	1.601	1.5972
5	2.4123	1.9802	1.8611	1.8122	1.7873	1.7729	1.7639	1.7577	1.7534
10	2.8234	2.2880	2.1447	2.0863	2.0568	2.0397	2.0289	2.0216	2.0165
15	2.9154	2.3558	2.2070	2.1465	2.1159	2.0982	2.0870	2.0794	2.0741
20	2.9490	2.3805	2.2297	2.1684	2.1374	2.1194	2.1081	2.1005	2.0951
30	2.9735	2.3985	2.2462	2.1843	2.1530	2.1349	2.1234	2.1158	2.1103
40	2.9822	2.4048	2.2520	2.1899	2.1585	2.1403	2.1289	2.1212	2.1157
50	2.9863	2.4078	2.2547	2.1925	2.1611	2.1429	2.1314	2.1237	2.1182
60	2.9884	2.4094	2.2562	2.1940	2.1625	2.1443	2.1328	2.1250	2.1196
70	2.9898	2.4103	2.2571	2.1948	2.1633	2.1451	2.1336	2.1259	2.1204
80	2.9906	2.4110	2.2576	2.1954	2.1639	2.1456	2.1341	2.1264	2.1209
90	2.9912	2.4114	2.2580	2.1958	2.1642	2.1460	2.1345	2.1268	2.1213
100	2.9916	2.4117	2.2583	2.1960	2.1645	2.1463	2.1348	2.1270	2.1215
1000	2.9934	2.4130	2.2595	2.1972	2.1656	2.1474	2.1359	2.1281	2.1227
1500	2.9934	2.4130	2.2595	2.1972	2.1656	2.1474	2.1359	2.1281	2.1227

**Table 6:** Percentage difference of buckling load on the CCFS rectangular plate between polynomial and trigonometric approach

$\alpha = \frac{a}{t}$	Average Percentage Difference %								
	$\beta = 1.0$	$\beta = 1.5$	$\beta = 2.0$	$\beta = 2.5$	$\beta = 3.0$	$\beta = 3.5$	$\beta = 4.0$	$\beta = 4.5$	$\beta = 5.0$
4	10.191	5.7982	2.7993	1.0098	0.0906	0.7961	1.2686	1.5994	1.8394
5	9.3083	5.3989	2.4712	0.7003	0.3916	1.0893	1.5571	1.8847	2.1224
10	7.9256	4.7864	1.9525	0.2008	0.8792	1.5682	2.0306	2.3546	2.5898
15	7.6358	4.6600	1.8433	0.0942	0.9835	1.6711	2.1326	2.4561	2.6909
20	7.5314	4.6147	1.8039	0.0556	1.0212	1.7083	2.1696	2.4928	2.7275
30	7.4558	4.5819	1.7753	0.0277	1.0485	1.7353	2.1964	2.5195	2.7541
40	7.4292	4.5703	1.7653	0.0178	1.0582	1.7448	2.2059	2.5289	2.7635
50	7.4168	4.5650	1.7606	0.0132	1.0627	1.7493	2.2103	2.5333	2.7679
60	7.4101	4.5621	1.7580	0.0107	1.0651	1.7517	2.2127	2.5357	2.7703
70	7.4060	4.5603	1.7565	0.0092	1.0666	1.7531	2.2141	2.5371	2.7717
80	7.4034	4.5592	1.7555	0.0083	1.0675	1.7541	2.2150	2.5381	2.7726
90	7.4016	4.5583	1.7548	0.0076	1.0682	1.7547	2.2157	2.5387	2.7733

100	7.4003	4.5578	1.7543	0.0071	1.0687	1.7552	2.2161	2.5392	2.7737
1000	7.3948	4.5555	1.7523	0.0051	1.0706	1.7572	2.2181	2.5411	2.7757
1500	7.3948	4.5554	1.7523	0.0051	1.0706	1.7572	2.2181	2.5411	2.7757
Average % difference	7.7803	4.7256	1.8970	0.1448	0.9342	1.6230	2.0854	2.4094	2.6446
Total Average % difference	2.6938								

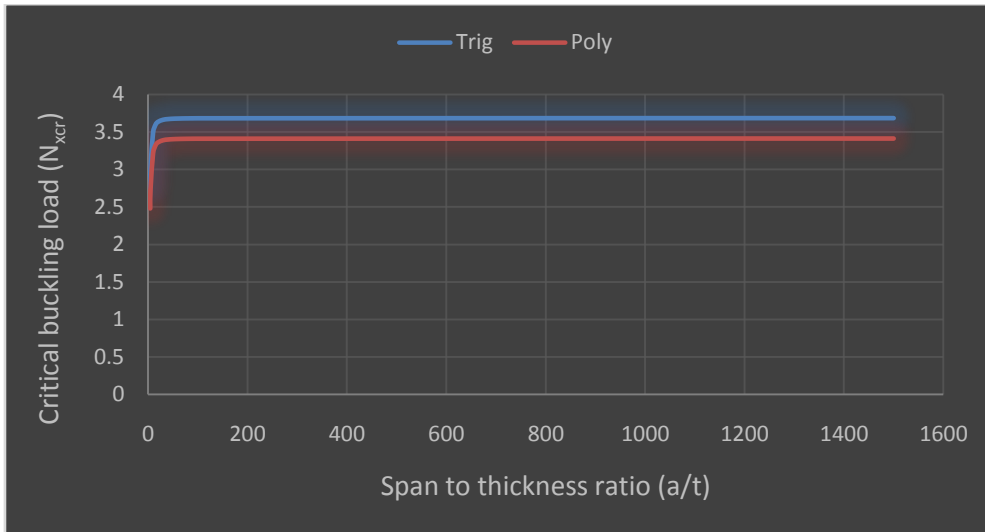


Figure 3: Graph of Critical buckling load ( $N_{xcr}$ ) versus aspect ratio ( $a/t$ ) of a square rectangular plate

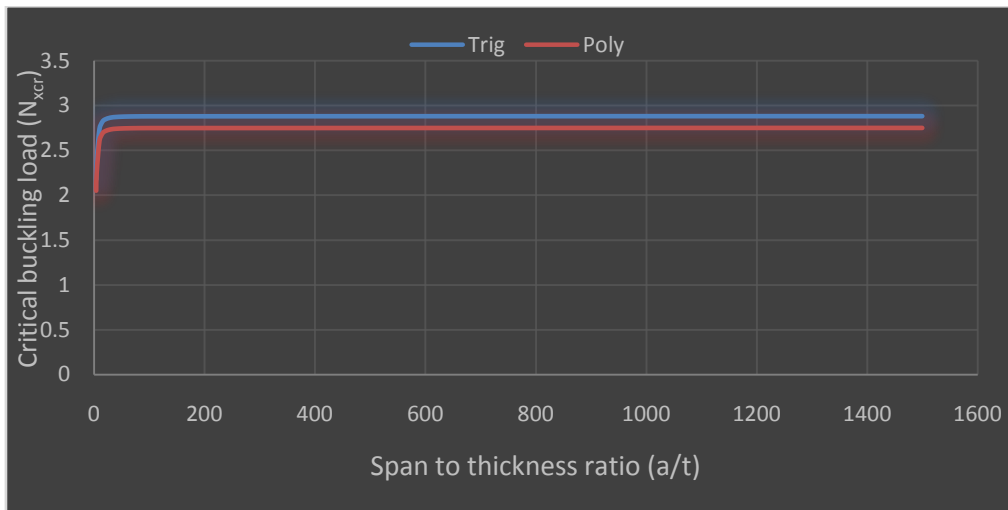
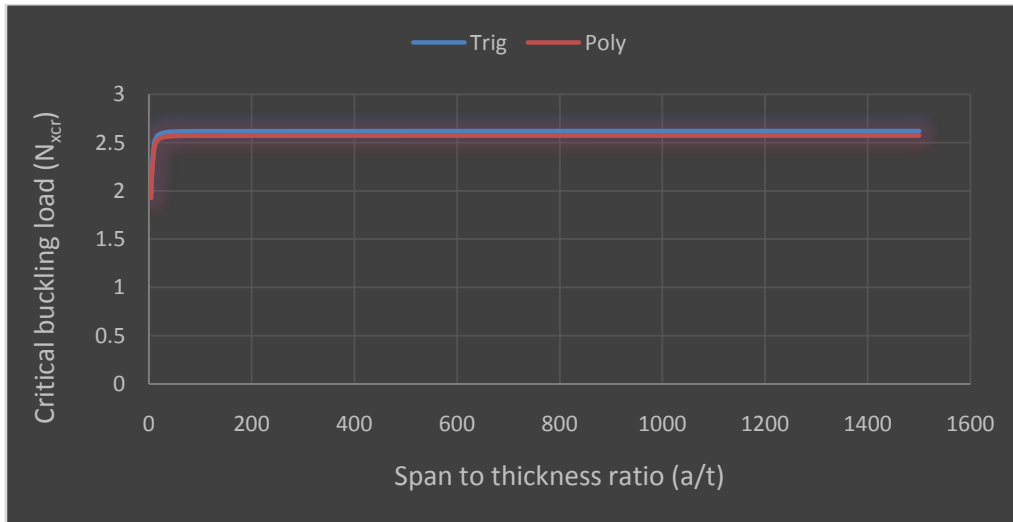
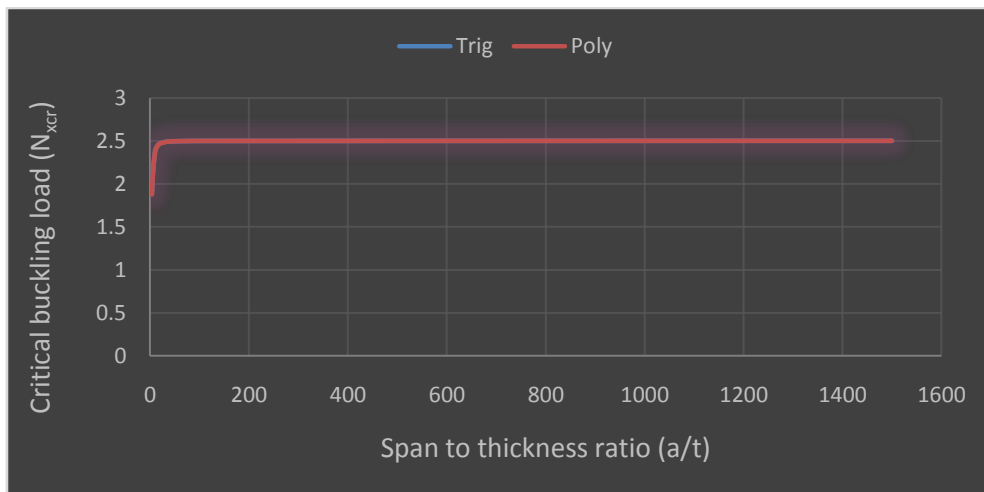


Figure 4: Graph of Critical buckling load ( $N_{xcr}$ ) versus aspect ratio ( $a/t$ ) of a rectangular plate with length to width ratio of 1.5.



**Figure 5:** Graph of Critical buckling load ( $N_{xcr}$ ) versus aspect ratio ( $a/t$ ) of a rectangular plate with length to width ratio of 2.0



**Figure 6:** Graph of Critical buckling load ( $N_{xcr}$ ) versus aspect ratio ( $a/t$ ) of a rectangular plate with length to width ratio of 2.5

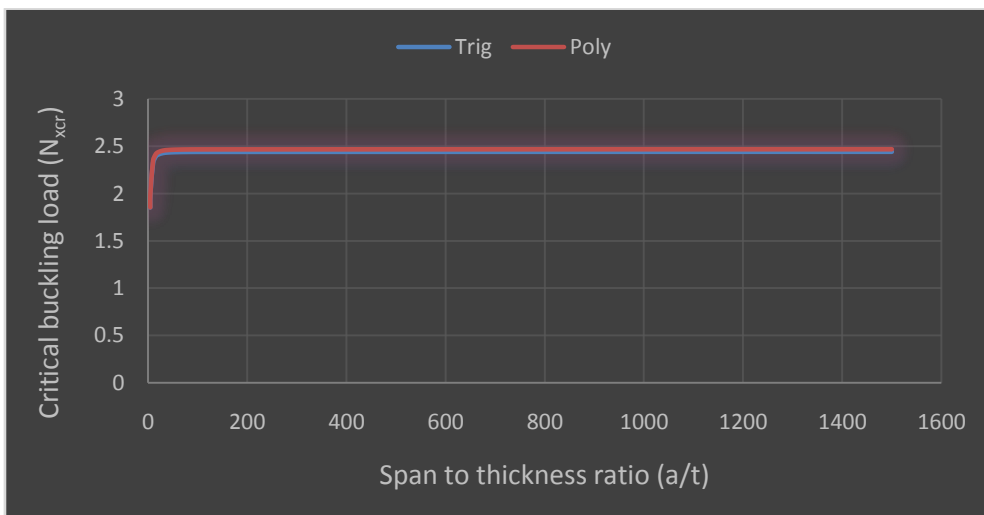


**Figure 7:** Graph of Critical buckling load ( $N_{xcr}$ ) versus aspect ratio ( $a/t$ ) of a rectangular plate with length to width ratio of 3.0

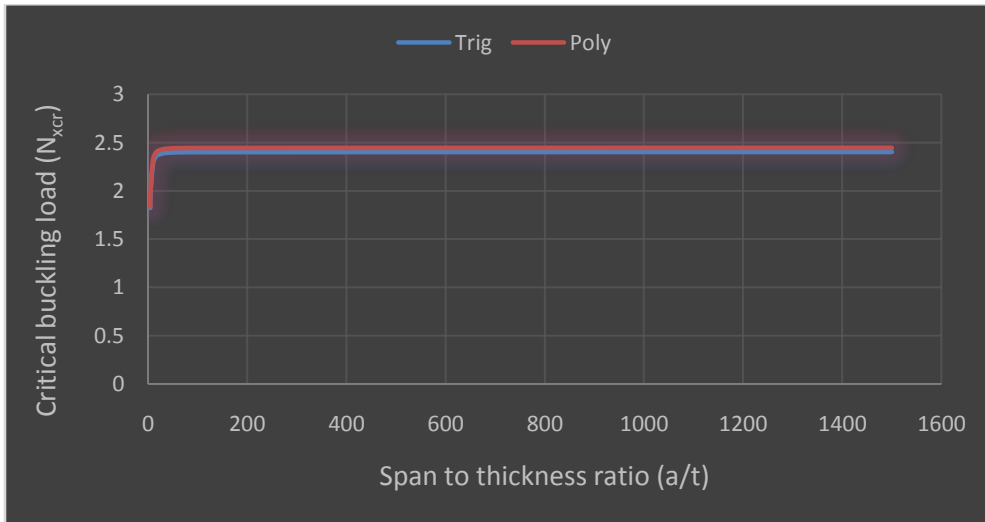


**Figure 8:** Graph of Critical buckling load ( $N_{xcr}$ ) versus aspect ratio ( $a/t$ ) of a rectangular plate with length to width ratio of 3.5

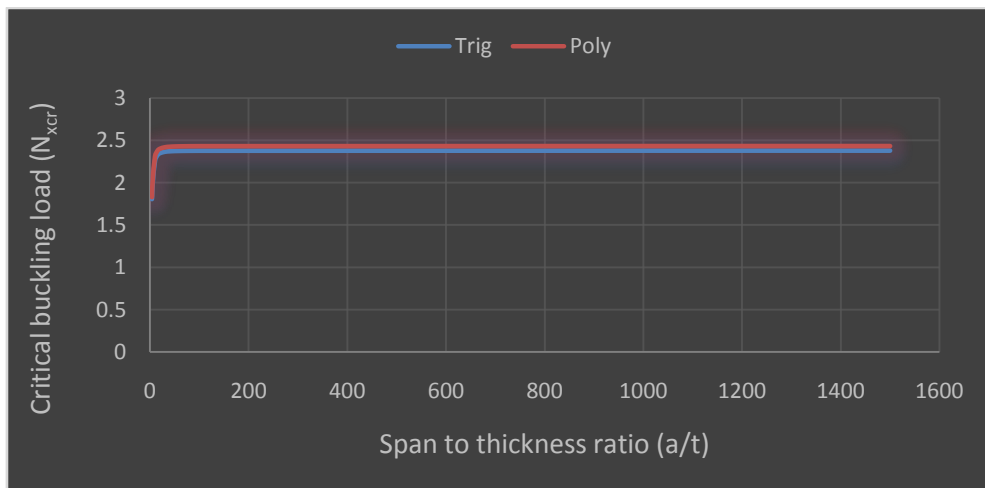


**Figure 9:** Graph of Critical buckling load ( $N_{xcr}$ ) versus aspect ratio ( $a/t$ ) of a rectangular plate with length to width ratio of 4.0

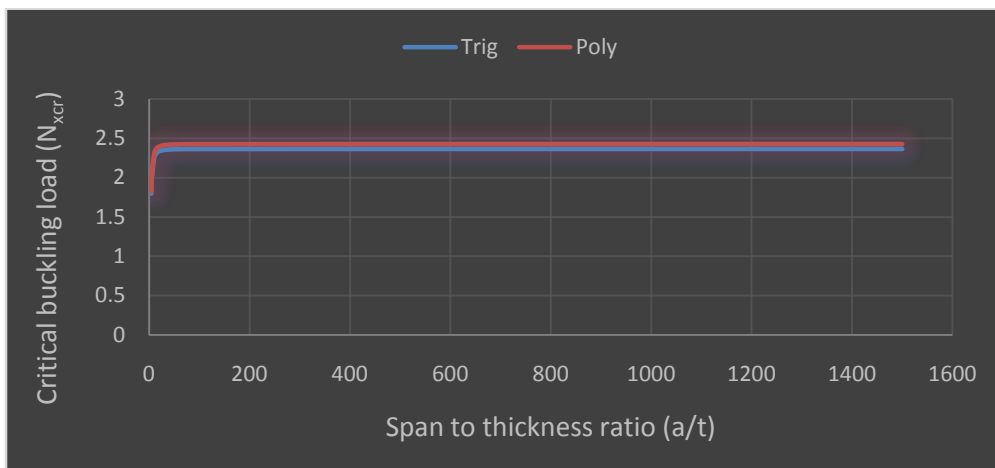


**Figure 10:** Graph of Critical buckling load ( $N_{xcr}$ ) versus aspect ratio ( $a/t$ ) of a rectangular plate with length to width ratio of 4.5

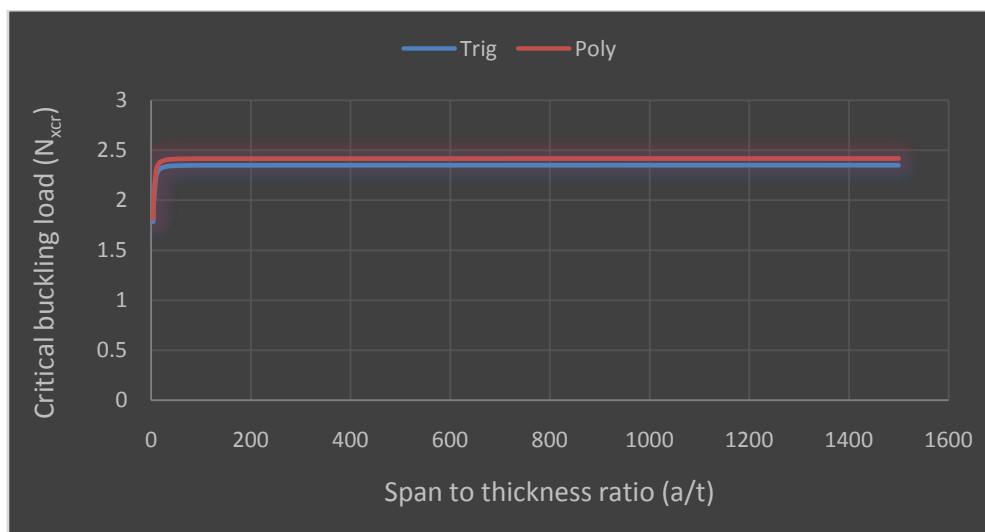


**Figure 11:** Graph of Critical buckling load ( $N_{xcr}$ ) versus aspect ratio ( $a/t$ ) of a rectangular plate with length to width ratio of 5.0

### References

- [1]. Onyeka, F. C., Ibearugbulem, O. M. (2020). Load Analysis and Bending Solutions of Rectangular Thick Plate. *International Journal on Emerging Technologies*, 11(3): 1103–1110.
- [2]. Onyeka, F. C., Edozie, O. T. (2020). Application of Higher Order Shear Deformation Theory in the Analysis of thick Rectangular Plate. *International Journal on Emerging Technologies*, 11(5): 62–67.
- [3]. Reddy, J.N. (2006). *Theory and Analysis of Elastic Plates and Shells*. CRC press
- [4]. Ibearugbulem, O. M. and Onyeka, F. C. (2020). Moment and stress analysis solutions of clamped rectangular thick plate. *European Journal of Engineering Research and Science*, 5(4): 531-534.
- [5]. Ezeh J. C., Onyechere I. C., Ibearugbulem O. M., Anya U. C. and Anyaogu L. (2018). Buckling Analysis of Thick Rectangular Flat SSSS Plates using Polynomial Displacement Functions. *International Journal of Scientific & Engineering Research*, 9(9): 387-392.
- [6]. Onyeka, F.C., Okafor, F.O. and Onah H.N. (2021). Application of a New Trigonometric Theory in the Buckling Analysis of Three-Dimensional Thick Plate. *International Journal of Emerging Technologies*. Vol.12(1): pp.228–240.
- [7]. Onyeka F. C., Okafor, F. O., Onah, H. N. (2018). Displacement and Stress Analysis in Shear Deformable Thick Plate. *International Journal of Applied Engineering Research*, 13(11): 9893-9908.
- [8]. Gunjal S.M., Hajare, R.B., Sayyad, A.S. & Ghodle, M.D. (2015). Buckling Analysis of Thick Plates using Refined Trigonometric Shear Deformation Theory. *Journal of Materials and Engineering Structures*, 2: 159–167.
- [9]. Onyeka, F.C., Okafor, F.O., Onah, H.N. (2019). Application of exact solution approach in the analysis of thick rectangular plate. *International Journal of Applied Engineering Research*, Vol. 14(8): 2043-2057.
- [10]. Sayyad, A.S. & Ghugal Y.M. (2012). Buckling analysis of thick isotropic plates by using exponential shear deformation theory. *Journal of Applied and Computational Mechanics*, 6: 185 – 196.
- [11]. Ibearugbulem, O. M., Ezeh, J. C., Nwadike, A. N., Maduh, U. J. (2014). Buckling Analysis of Isotropic SSSS Rectangular Plate using Polynomials Shape Function. *International Journal of Emerging Technology and Advanced Engineering*, 4 (1): 6-9.
- [12]. Onah H. N., Nwoji C.U., Ike C.C., Mama B.O. (2018). Elastic buckling analysis of uniaxially compressed CCSS Kirchhoff plate using single finite Fourier sine integral transform method. *International Information and Engineering Technology Association. Modelling, Measurement and Control B*, 87(2): 107-111.
- [13]. Onwuka D. O., Iwuoha S. E. (2017). Elastic instability analysis of biaxially compressed flat rectangular isotropic all-round clamped (CCCC) plates. *MOJ Civil Eng*, 2(2):52–56. DOI: 10.15406/mojce.2017.02.00027
- [14]. Ibearugbulem, O.M., Adah, E. I., Onwuka, D. O., Okere, C. E. (2020). Simple and Exact Approach to Post Buckling Analysis of Rectangular Plate. *SSRG International Journal of Civil Engineering (SSRG-IJCE)*, 7(6): 54-64
- [15]. Gunjal S. M., Hajare R.B, Sayyad A. S., Ghodle M.D. (2015). Buckling analysis of thick plates using refined trigonometric shear deformation theory. *Journal of Materials and Engineering Structures*, 2: 159–167.
- [16]. Onyeka, F.C., Okeke T. E and Wasiu, J. (2020). Strain–Displacement Expressions and their Effect on the Deflection and Strength of Plate. *Advances in Science, Technology and Engineering Systems*, 5(5): 401-413.
- [17]. Ibearugbulem, O.M, Ibeabuchi, V.T. and Njoku, K.O. (2014): Buckling analysis of SSSS stiffened rectangular isotropic plates using work principle approach. *International Journal of Innovative Research & Development*, 3(11): 169-176.
- [18]. Shufrin and Eisenberger, M. (2005). Stability and vibration of shear deformable plates - First order and higher order analyses. *International Journal of Solids and Structures*, 42(3-4): 1225–1251.
- [19]. Onyeka, F.C., Okafor, F.O. and Onah H.N. (2021). Application of a New Trigonometric Theory in the Buckling Analysis of Three-Dimensional Thick Plate. *International Journal of Emerging Technologies*, 12(1): 228–240.
- [20]. Onyeka, F. C., Okafor, F.O., Onah, H.N. (2021). Buckling Solution of a Three-Dimensional Clamped Rectangular Thick Plate Using Direct Variational Method. *IOSR Journal of Mechanical and Civil Engineering (IOSR-JMCE)*, 18(3): 10-22.
- [21]. Onyeka, F.C., Mama, B.O., Okeke, T.E. (2022). Exact three-dimensional stability analysis of plate using a direct variational energy method. *Civil Engineering Journal*, Vol. 8(1): 60–80.